J Mater Sci (2011) 46:6162–6167
DOI 10.1007/s10853-011-5679-1

LETTER

Continuous direct melt foaming of a preceramic polymer using carbon dioxide: extrusion device and first results

Friedrich Wolff · Helmut Münstedt

Received: 18 April 2011 / Accepted: 31 May 2011 / Published online: 11 June 2011

Introduction

In comparison to bulk materials, foams offer advantageous properties like low density, large surface area, high permeability, and low thermal conductivity. Therefore, foams are widely used in, e.g. thermal insulation, lightweight constructions, filtering, and catalysis. Prominent features of ceramic foams are high strength and stiffness, high temperature resistance, and high thermal shock resistance [1]. However, the foam properties depend strongly on the foam morphology and porosity which are influenced by the processing technique. The most important production routes incorporating preceramic polymers are the replica method, the template method, and direct foaming. The replica method uses an open cell polymer foam which is coated by a preceramic polymer slurry and subsequently pyrolysed leading to a positive foam structure [2–6]. The template method is based on organic phases such as polymer microbeads or expendable microspheres mixed into a preceramic polymer and decomposed during pyrolysis leading to a negative foam structure [7–18]. In the literature, there are also reports on combinations of the replica method and direct foaming [6] and the template method and direct foaming [19–21]. The direct foaming approach can be classified in (a) physical foaming [22–25], (b) chemical foaming [26–31], and (c) a combination of physical and chemical foaming by co-blowing the preceramic polymer together with polyurethane [30, 32–37]. In chemical foaming, either a suitable chemical foaming agent has to be found or the blowing is caused by volatile condensation products during crosslinking. In the latter case, however, the amount of "blowing agent" being available is given by the molecular structure of the preceramic polymer and the gas production is directly coupled with the crosslinking process.

Physical foaming has the big advantage that the content of added foaming agent can be varied independently of other parameters and, therefore, a wide range for the variation of parameters like temperature or pressure is available.

Up to now, pure physical foaming of preceramic polymers has only been carried out in a batch process using carbon dioxide as foaming agent [22–25]. In this process, the material is saturated in an autoclave with carbon dioxide under high pressure. Subsequently, the foaming is initiated by a rapid pressure drop causing a thermodynamic instability.

Continuous foaming of preceramic polymers melts using an extrusion process has only been carried out with the template method, so far [14]. The reason for this deficit is due to the difficult processing of the preceramic polymers. Although the material displays thermoplastic behaviour in the uncrosslinked state, the viscoelastic properties differ from those of common engineering polymers due to the absence of chain entanglements, the low glass transition temperature, and the high temperature dependence of the viscoelastic properties [38]. In this article, the continuous physical extrusion foaming of a preceramic polymer melt is described for the first time. For this purpose, extrusion combined with physical foaming which is well known for organic thermoplasts [e.g. 39–43] was adapted to the shaping of preceramic polymer foams. Applying carbon dioxide, this process can be considered as

---

F. Wolff · H. Münstedt (✉)
Department of Materials Science, Institute of Polymer Materials,
Friedrich-Alexander-University Erlangen-Nürnberg,
Martensstr 7, 91058 Erlangen, Germany
e-mail: helmut.muenstedt@ww.uni-erlangen.de

an economic and environmentally friendly method of foam production.

The process presented offers the possibility to produce a large quantity of foams with a variety of foam morphologies. By changing the die geometry different profiles of foamed items are accessible.

Experimental

The material used is a commercially available methyl silicone resin, or more precisely, a polymethylsilsesquioxane. It is available on the market under the trade name Silres MK from Wacker Chemie AG, Germany. The silicone resin with the elemental formula $(CH_3–SiO_{1.5})_n$ possesses a highly branched molecular structure (Fig. 1) with a weight average molar mass of about 8,000 g/mol. The molecules contain a certain amount of functional side groups (hydroxyl and ethoxy groups) which can provide a further condensation of this material [cf. 38]. The products of this condensation reaction are water and ethanol.

The material is solid at room temperature with a glass transition temperature of 51 °C and is provided as a powder. A granulate with a maximum size of 2 mm was made from the powder by slightly melting it together to sheets and subsequently breaking it into pieces. 1 wt% talcum was distributed on the surface as a processing aid. In order to facilitate a crosslinking of the silicone resin foam 0.5 wt% zinc acetylacetonate (ZnAcAc) was added as a catalyst. This crosslinking is essential for the production of ceramic foams since otherwise the material melts and the foam structure collapses during pyrolysis.

The foam extrusion line (Fig. 2) consists of a single-screw extruder (Extrusiograph 30/25D, Brabender, Germany), a continuously working high pressure syringe pump (Isco 260D, Teledyne Isco, USA), a static mixer with heat exchanger (custom unit), a die, and a conveyor belt. The extruder has a three-section screw with a diameter of 30 mm, the *L*/*D* ratio is 25. The total length of the static mixer heat exchanger unit is about 300 mm and the conveyor belt is about 1.2 m long with a width of 60 mm. For this study, a circular die with a diameter of 2 mm was used. The melt temperature and pressure can be measured at several positions along the extrusion line including the die.

The carbon dioxide is injected into the melt stream in front of the static mixer. During passing it, the carbon dioxide is dissolved in the molten silicone resin. The temperature during mixing can be controlled by the heat exchanger. At the die, the pressure is released, the preceramic polymer foams, and the foamed strand is conveyed by the belt which is made from glass fibre reinforced PTFE which is able to withstand temperatures up to 250 °C (Fig. 3). The specifications of the device cover a broad scale (cf. Table 1). However, only a particular range was applicable for the processing of the silicone resin. The data

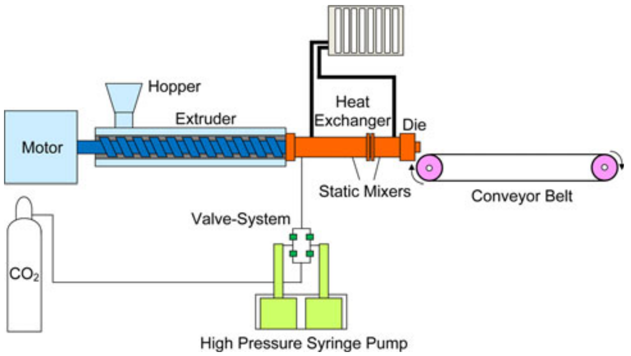

Fig. 2 Schematic of the foam extrusion line for silicone resins

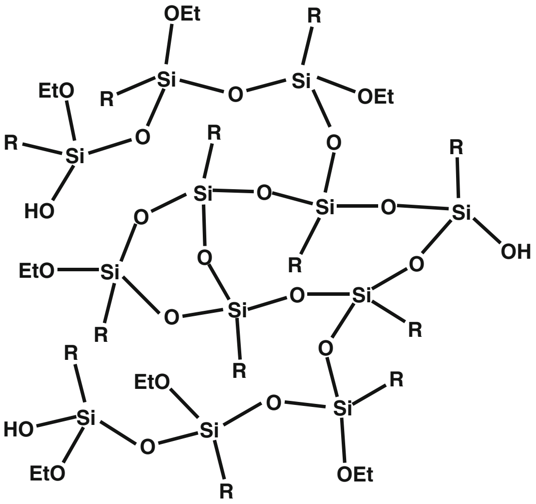

Fig. 1 Schematic of the molecular structure of the silicone resin. *R* represents methyl groups

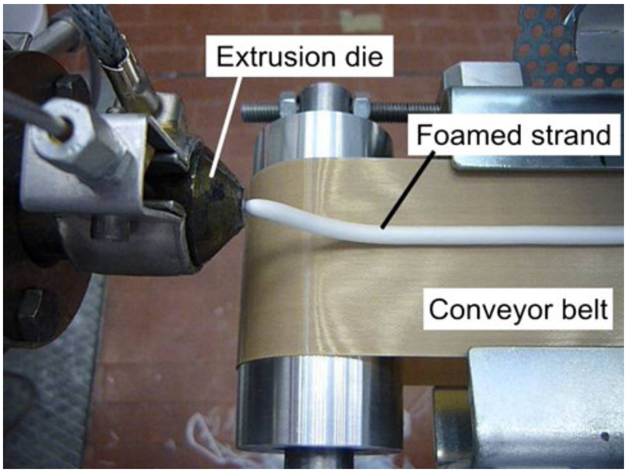

Fig. 3 Photography of a foamed silicone resin strand during extrusion

Table 1 Specifications of the foam extrusion line and experimental settings used

	General specifications	Range for silicone resins	Parameters used
Foaming temperature (°C)	Up to 220	70–100	87
Screw rotational frequency (min^{-1})	Up to 120	10–30	15
Throughput (kg/h)	Up to 15	1.5–5.0	2.8
Flow rate of CO_2 pump (mL/min)	0.001–107	0.2–2.0	0.5
Pressure of CO_2 pump (bar)	0.7–517	50–150	58

are listed in Table 1 together with the experimental parameters used for Silres MK in this article.

Results and discussion

The foamed strands obtained possess a gradient pore structure with closed cells dominating (Fig. 4). Since the cooling of the material is comparatively fast at the rim, the bubble growth is stopped there in an early stage, whereas the strand cools down much more slowly in the middle of the strand. Hence, the bubbles in the center of the strands can grow to bigger pore sizes and even some open cells can be found. The heat transfer in the foaming material is very complex since the foam morphology permanently changes until the foam is stabilised and the foam is insulating itself. Due to this fact and the pronounced temperature gradient, a modelling of the cooling behaviour and the foam structure will be very challenging.

The foamed strand depicted in Fig. 4 was obtained at a foaming temperature of 87 °C and a foaming pressure of 27 bar using a carbon dioxide concentration of approximately 1.2 wt%. In this case, a pore size gradient from more than 200 µm in the middle to smaller than 20 µm at the rim was found. The average pore size was 61 µm and the overall density measured according to the Archimedes principle was 0.27 ± 0.01 g/cm^3. This is equivalent to a porosity of $79 \pm 1\%$. The average cell density is 5.5×10^5 cm^{-3}.

In order to quantify the gradient a coordinate system was introduced into the SEM images as it is shown for the cross-section in Fig. 5 and for the longitudinal section in Fig. 6. Hence, every single pore can be related to a set of coordinates. For the reason of clarity, the distance from the middle to the rim was classified in ten classes and an average pore size was determined for each class. The central class contains only three pores whereas the average pore size of the class close to the rim was obtained from more than 200 pores. In case of the longitudinal section, the average pore size value was calculated from six to 30 pores for the radial analysis and about ten pores for the analysis in extrusion direction.

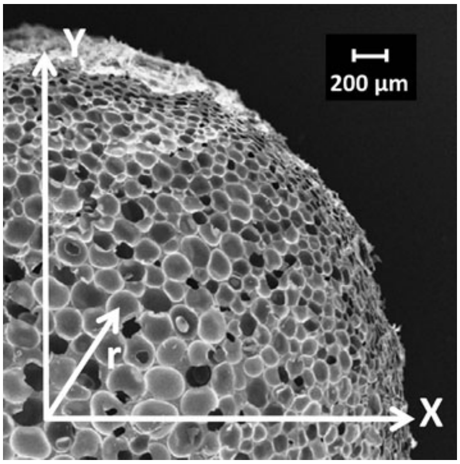

Fig. 5 Scanning electron micrograph with the coordinate system chosen of a cross-section of a foamed silicone resin strand obtained at 87 °C and 27 bar with a carbon dioxide concentration of approx. 1.2 wt%

The average pore size of the cross-section in dependence on the relative distance from the center of the sample is shown in Fig. 7 in which the bars reflect the distribution of

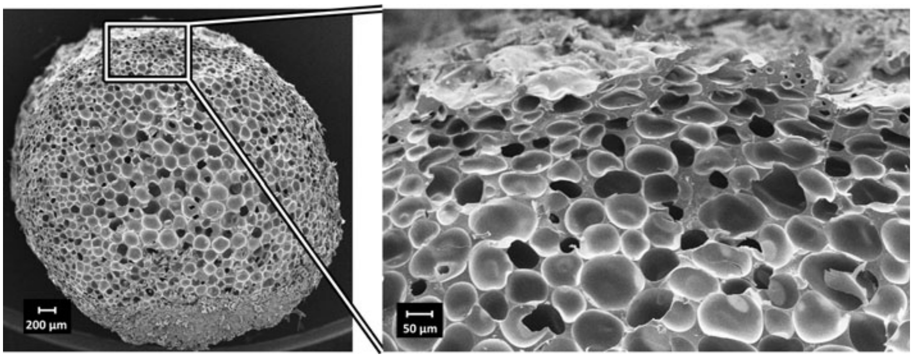

Fig. 4 Scanning electron micrograph of the cross-section of a foamed silicone resin strand. The foaming was carried out at 87 °C and 27 bar with a carbon dioxide concentration of approx. 1.2 wt%

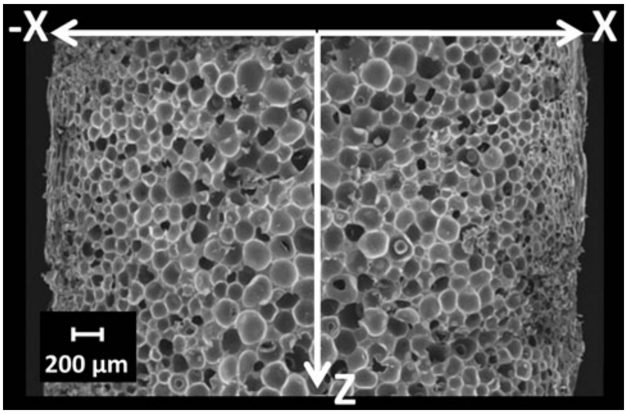

Fig. 6 Scanning electron micrograph with the coordinate system of a longitudinal section of a foamed silicone resin strand obtained at 87 °C and 27 bar with a carbon dioxide concentration of approx. 1.2 wt%

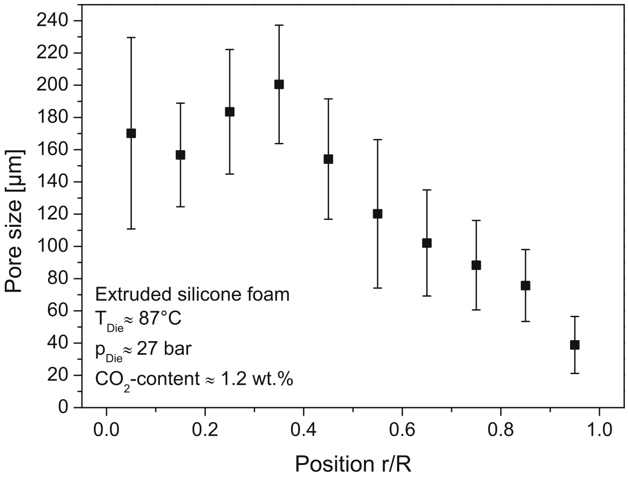

Fig. 7 Average pore sizes of the cross-section in dependence on the relative distance from the center. The radius of the extruded strand *R* was about 2 mm

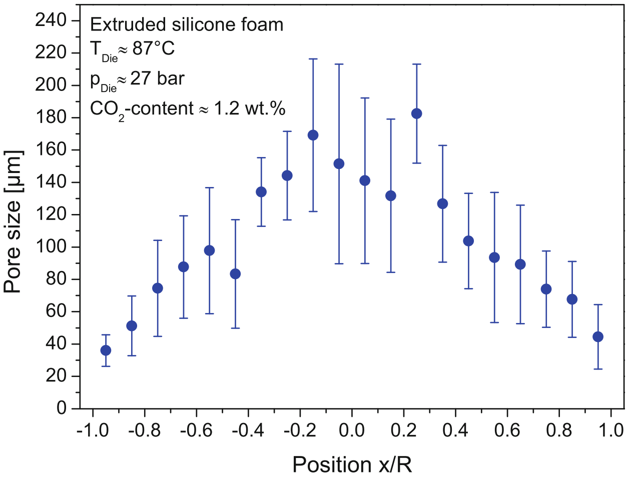

Fig. 8 Average pore sizes of the longitudinal section in dependence on the relative distance from the center. The radius of the extruded strand *R* was about 2 mm

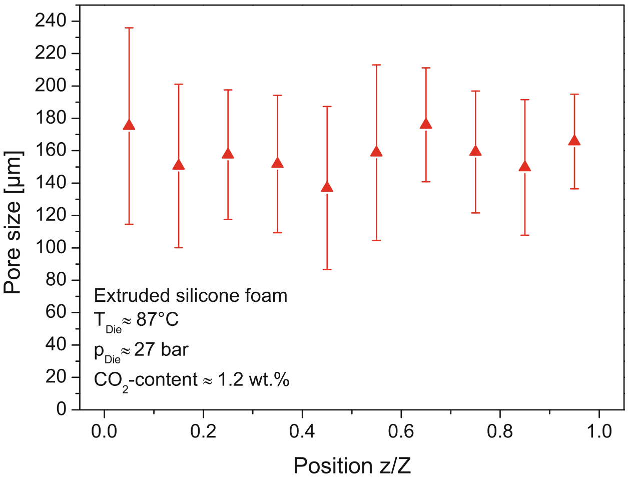

Fig. 9 Average pore sizes of the longitudinal section in dependence of the relative position along the extrusion direction. The analysed length *Z* was 3 mm

the pore size in each class. Up to the relative distance of 0.3 from the center, the average pore size is nearly constant. From 0.3 to 1.0 relative distance the average pore size becomes smaller. At the rim, average pore sizes of around 40 µm are obtained.

In case of the longitudinal section, the symmetry of the pore size gradient in radial direction is clearly visible (Fig. 8), whereas along the extrusion axis the average pore size is approximately constant (Fig. 9). For the analysis of the average pore size along the extrusion axis only the pores within a maximum relative distance of one quarter from the center of the sample were taken since it was shown that in this region no pore size gradient exists (cf. Figs. 7, 8).

In order to prove this concept of fabricating ceramic foams the foamed silicone resins were crosslinked and subsequently pyrolysed. The crosslinking was performed in a two step process in which, first, the foam structure was stabilised applying a $SiCl_4$ vapour treatment at room temperature. Subsequently, the foams can be crosslinked thermally. For that purpose, the temperature was increased stepwise to 70, 100, and 120 °C. The pyrolysis was performed at the Institute of Glass and Ceramics at the University Erlangen-Nürnberg in a nitrogen atmosphere at 800 °C. The SEM image of the ceramic foam obtained shows that the foam morphology is not changed apart from the shrinkage that is inherent to the conversion of a preceramic polymer to a ceramic material (Fig. 10). More details on the pyrolysis and the produced ceramic foams will be published elsewhere.

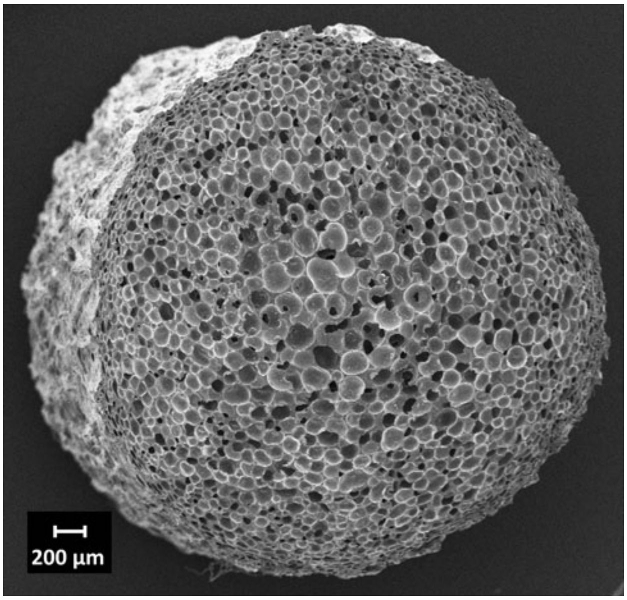

Fig. 10 Scanning electron micrograph of a ceramic foam obtained by pyrolysis of a silicone resin foam at 800 °C in a nitrogen atmosphere

Conclusion

A continuously working foam extrusion line for preceramic polymers was set up on a technical scale. Porosities of about 80% were obtained for foams showing a gradient pore structure from about 200 µm in the center region to 20 µm at the rim of the strand. The design of the foam extrusion line with exchangeable dies would make different profile geometries feasible. A big advantage of the concept presented is the high degree of freedom with respect to the processing conditions. As an example the content of blowing agent can be set independently of other parameters. Therefore, this processing method is applicable for an economic and ecological production of silicone resin foams which can be used as precursors for ceramic foams but also for high temperature applications (e.g. insulation, fire protection) of the non-pyrolysed material. Open cell ceramic foams which are desired for some applications might be feasible by using higher CO_2 concentrations or adding organic additives to the silicone resin which do not foam but decompose during pyrolysis and lead to the formation of cell windows.

Acknowledgements The authors gratefully acknowledge the funding of the German Research Foundation (DFG), which, within the framework of its "Excellence Initiative" supports the Cluster of Excellence "Engineering of Advanced Materials" (www.eam.uni-erlangen.de) at the University Erlangen-Nuremberg. Special thanks go to Dr. Larissa Zirkel and Dr. Joachim Kaschta for their helpful discussions and suggestions during the set up of the foam extrusion line. The support of the Institute of Glass and Ceramics of the University Erlangen-Nürnberg at which the pyrolysis of the sample shown was performed, is highly acknowledged.

References

1. Kumar BVM, Kim Y-W (2010) Sci Technol Adv Mater 11:044303
2. Bao X, Nangrejo MR, Edirisinhe MJ (2000) J Mater Sci 35:4365. doi:10.1023/A:1004805023228
3. Nangrejo MR, Bao X, Edirisinghe MJ (2000) J Eur Ceram Soc 20:1777
4. Nangrejo MR, Bao X, Edirisinghe MJ (2000) J Mater Sci Lett 19:787
5. Nangrejo MR, Edirisinghe MJ (2002) J Porous Mat 9:131
6. Ceron-Nicolat B, Fey T, Greil P (2010) Adv Eng Mater 12:884
7. Colombo P, Bernardo E (2003) Compos Sci Technol 63:2353
8. Colombo P, Bernardo E, Biasetto L (2004) J Am Ceram Soc 87:152
9. Shibuya M, Sakurai M, Takahashi T (2007) Compos Sci Technol 67:3338
10. Shibuya M, Takahashi T, Koyama K (2007) Comps Sci Technol 67:119
11. Kim Y-W, Kim S-H, Kim H-D, Park CB (2004) J Mater Sci 39:5647. doi:10.1023/B:JMSC.0000040071.55240.85
12. Kim Y-W, Jin Y-J, Chun Y-S, Song I-H, Kim H-D (2005) Scr Mater 53:921
13. Kim Y-W, Kim S-H, Song I-H, Kim H-D, Park CB (2005) J Am Ceram Soc 88:2949
14. Kim Y-W, Eom J-H, Wang C, Park CB (2008) J Am Ceram Soc 91:1361
15. Kim Y-W, Jin Y-J, Eom J-H, Song I-H, Kim H-D (2010) J Mater Sci 45:2808. doi:10.1007/s10853-010-4270-5
16. Biasetto L, Francis A, Palade P, Principi G, Colombo P (2008) J Mater Sci 43:4119. doi:10.1007/s10853-007-2224-3
17. Jang D-H, Kim Y-W, Song I-H, Kim H-D, Park CB (2006) J Ceram Soc Jpn 114:549
18. Kumar BVM, Zhai W, Eom J-H, Kim Y-W, Park CB (2011) J Mater Sci 46:3664. doi:10.1007/s10853-011-5284-3
19. Wang C, Wang J, Park CB, Kim Y-W (2007) J Mater Sci 42:2854. doi:10.1007/s10853-006-0229-y
20. Kim Y-W, Wang C, Park CB (2007) J Ceram Soc Jpn 115:419
21. Eom J-H, Kim Y-W (2007) Met Mater Int 13:521
22. Kim Y-W, Kim S-H, Xu X, Choi C-H, Park CB, Kim H-D (2002) J Mater Sci Lett 21:1667
23. Kim Y-W, Kim S-H, Wang C, Park CB (2003) J Am Ceram Soc 86:2231
24. Kim Y-W, Park CB (2003) Compos Sci Technol 63:2371
25. Wolff F, Zirkel L, Betzold S, Jakob M, Maier V, Nachtrab F, Ceron-Nicolat B, Fey T, Münstedt H (2011) Int Polym Proc. doi:10.3139/217.2469
26. Takahashi T, Colombo P (2003) J Porous Mater 10:113
27. Kim Y-W, Lee K-H, Lee S-H, Park CB (2003) J Ceram Soc Jpn 111:863
28. Zeschky J, Goetz-Neunhoeffer F, Neubauer J, Jason Lo SH, Kummer B, Scheffler M, Greil P (2003) Compos Sci Technol 63:2361
29. Zeschky J, Höfner T, Arnold C, Weißmann R, Bahloul-Hourlier D, Scheffler M, Greil P (2005) Acta Mater 53:927
30. Colombo P, Gambaryan-Roisman T, Scheffler M, Buhler P, Greil P (2001) J Am Ceram Soc 84:2265
31. Rocha RM, Moura EAB, Bressiani AHA, Bressiani JC (2008) J Mater Sci 43:4466. doi:10.1007/s10853-008-2654-6
32. Colombo P, Griffoni M, Modesti M (1998) J Sol-Gel Sci Technol 13:195
33. Colombo P, Modesti M (1999) J Sol-Gel Sci Technol 14:103
34. Colombo P, Modesti M (1999) J Am Ceram Soc 82:573
35. Takahashi T, Münstedt H, Colombo P, Modesti M (2001) J Mater Sci 36:1627. doi:10.1023/A:1017531415890

36. Takahashi T, Münstedt H, Modesti M, Colombo P (2001) J Eur Ceram Soc 21:2821
37. Schmidt H, Koch D, Grathwohl G, Colombo P (2001) J Am Ceram Soc 84:2252
38. Wolff F, Kugler C, Münstedt H (2010) Rheol Acta. doi: 10.1007/s00397-010-0513-2
39. Park CB, Behravesh AH, Venter RD (1998) Polym Eng Sci 38:1812
40. Sauceau M, Nikitine C, Rodier E, Fages J (2007) J Supercrit Fluid 43:367
41. Nikitine C, Rodier E, Dauceau M, Letourneau J–J, Fages J (2010) J Appl Polym Sci 115:981
42. Han X, Koelling KW, Tomasko DL, Lee LJ (2002) Polym Eng Sci 42:2094
43. Siripurapu S, Gay YJ, Royer JR, De Simone JM, Spontak RJ, Khan SA (2002) Polymer 43:5511